The HIV-1 Viral Protein R Induces Apoptosis via a Direct Effect on the Mitochondrial Permeability Transition Pore

By Etienne Jacotot,* Luigi Ravagnan,* Markus Loeffler,* Karine F. Ferri,* Helena L.A.Vieira,* Naoufal Zamzami,* Paola Costantini,* Sabine Druillennec,‡ Johan Hoebeke,§ Jean Paul Briand,§ Theano Irinopoulou,‖ Eric Daugas,* Santos A. Susin,* Denis Cointe,¶ Zhi Hua Xie,** John C. Reed,** Bernard P. Roques,‡ and Guido Kroemer*

*From *Centre National de la Recherche Scientifique, F-94801 Villejuif, France; ‡Unité de Pharmacochimie Moléculaire et Structurale, Institut National de la Santé et de Recherche Médicale (INSERM) U266, CNRS UMR 860, Université René Descartes (Paris V), 75006 Paris, France; §Institut de Biologie Moléculaire et Cellulaire, Centre National de la Recherche Scientifique, 67084 Strasbourg, France; ‖INSERM U430, Broussais Hospital, 75014 Paris, France; ¶Laboratoire de Virologie et Immunologie, Hopital Antoine Beclère, 92141 Clamart, France; and **The Burnham Institute, La Jolla, California 92037*

Abstract

Viral protein R (Vpr) encoded by HIV-1 is a facultative inducer of apoptosis. When added to intact cells or purified mitochondria, micromolar and submicromolar doses of synthetic Vpr cause a rapid dissipation of the mitochondrial transmembrane potential ($\Delta\Psi_m$), as well as the mitochondrial release of apoptogenic proteins such as cytochrome *c* or apoptosis inducing factor. The same structural motifs relevant for cell killing are responsible for the mitochondriotoxic effects of Vpr. Both mitochondrial and cytotoxic Vpr effects are prevented by Bcl-2, an inhibitor of the permeability transition pore complex (PTPC). Coincubation of purified organelles revealed that nuclear apoptosis is only induced by Vpr when mitochondria are present yet can be abolished by PTPC inhibitors. Vpr favors the permeabilization of artificial membranes containing the purified PTPC or defined PTPC components such as the adenine nucleotide translocator (ANT) combined with Bax. Again, this effect is prevented by addition of recombinant Bcl-2. The Vpr COOH terminus binds purified ANT, as well as a molecular complex containing ANT and the voltage-dependent anion channel (VDAC), another PTPC component. Yeast strains lacking ANT or VDAC are less susceptible to Vpr-induced killing than control cells yet recover Vpr sensitivity when retransfected with yeast ANT or human VDAC. Hence, Vpr induces apoptosis via a direct effect on the mitochondrial PTPC.

Key words: apoptosis • Bcl-2 • cell death • mitochondria • Vpr

Introduction

AIDS is associated with an enhanced apoptotic decay of various cell types, in particular lymphocytes, monocytes, and neurons. The mechanisms of this deregulated cellular turnover are complex and involve host factors, direct viral effects, and soluble viral proteins including gp120, Tat, Nef, and viral protein R (Vpr)[1] (1–4). Although none of these mechanisms or factors, taken on their own, can explain the AIDS-associated depletion of important cell types, it appears important to understand their function individually. The 14-kD protein Vpr is abundant in virions (3, 5) and is detectable in the sera of HIV-1 carriers, correlating with the viral load (6). Vpr is likely to be important for AIDS pathogenesis, and loss-of-function mutations of Vpr are negatively selected in vivo (7). Vpr interacts with multiple intracellular targets and has pleiotropic effects on viral replication, cell cycle, and differentiation (3, 5). In addition,

Address correspondence to Guido Kroemer, 19 rue Guy Môquet, B.P. 8, F-94801 Villejuif, France. Phone: 33-1-49-58-35-13; Fax: 33-1-49-58-35-09; E-mail: kroemer@infobiogen.fr

[1]*Abbreviations used in this paper:* AIF, apoptosis inducing factor; ANT, adenine nucleotide translocator; Atr, atractyloside; BA, bongkrekic acid; COX, cytochrome *c* oxidase; CsA, cyclosporin A; PI, propidium iodide; PTPC, permeability transition pore complex; RT, room temperature; VDAC, voltage-dependent anion channel; Vpr, viral protein R.

Vpr kills lymphocytes (8), monocytes (9), and neurons (10), either upon infection with *vpr*-positive HIV-1 isolates (8, 9) or upon extracellular addition of the Vpr protein (10, 11). Intrigued by the pleiotropic cytotoxic potential of Vpr, we decided to explore the apoptogenic mode of action of this HIV-1 accessory protein.

Apoptosis research has recently been boosted by the development of cell-free systems in which isolated organelles (nuclei, mitochondria, cytosol, etc.) are coincubated in vitro (12–19). This approach has generated evidence that mitochondrial intermembrane proteins, including cytochrome *c*, apoptosis inducing factor (AIF), procaspases, and heat shock proteins, are released during apoptosis and are crucial for the activation of caspases and DNases (17–23). The mechanism responsible for mitochondrial membrane permeabilization has been found to involve proapoptotic members of the Bcl-2 family (Bax, Bak, Bid, etc.; reference 24–28) and/or the permeability transition pore complex (PTPC), a polyprotein complex organized around the two most abundant proteins of the inner and outer mitochondrial membranes, the adenine nucleotide translocator (ANT; inner membrane) and the voltage-dependent anion channel (VDAC; outer membrane). ANT, VDAC, Bcl-2, and Bax physically interact within the inner–outer membrane contact site (27–30). Cell-free systems also allow mapping of the site of action of xenobiotic apoptosis inducers. Schematically, two classes of inducers can be distinguished. First, a variety of different inducers act directly on mitochondria and/or purified PTPC. This is true for experimental anticancer agents such as lonidamine (31), betulinic acid (32), arsenite (33), and diamide (34), as well as for toxins such as salicylate (35) and mastoparan (16). In contrast, the majority of apoptosis inducers act indirectly on mitochondria, e.g., via triggering of the ceramide pathway, increases in Ca^{2+} levels, effects on the subcellular distribution of proteins from the Bcl-2/Bax family, caspase activation, or shifts in redox potentials, which then affect the PTPC (and perhaps alternative permeabilization mechanisms (16, 24–28, 36–38).

Based on the above premises, we decided to elucidate the apoptogenic mode of action of Vpr, both in cells and in cell-free systems. Our results indicate that Vpr can directly target mitochondrial PTPC and permeabilize mitochondrial membranes in cell-free systems. Moreover, Vpr can act on purified PTPC or PTPC components reconstituted into synthetic membranes. Cell lacking key proteins from the PTPC become relatively resistant to the cytotoxic effect of Vpr. Thus, Vpr represents a novel type of viral peptide that can interact with the PTPC to permeabilize mitochondrial membranes and trigger the apoptotic program.

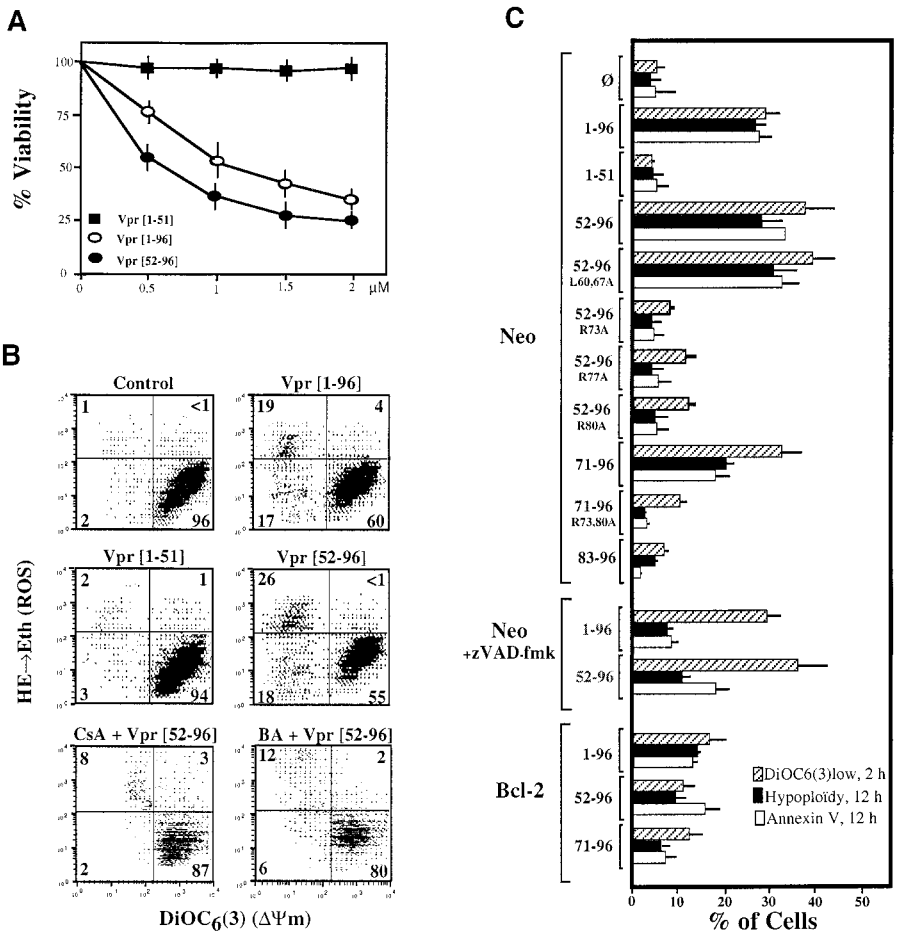

Figure 1. Proapoptotic effects of Vpr and Vpr-derived peptides (35). (A) Cytocidal effects of Vpr on Jurkat cells. After overnight incubation, plasma membrane permeability was assessed by PI staining. This experiment was reproduced five times. (B) Acute mitochondrial Vpr effects. Jurkat cells were cultured for 2 h with 0.5 μM Vpr52-96, 1 μM Vpr1-96, 1 μM Vpr1-51, 10 μM CsA, and/or 50 μM BA, followed by staining with $\Delta\Psi_m$-sensitive $DiOC_6(3)$ and hydroethidine (HE), which reacts with superoxide anion to the fluorochrome ethidium (Eth). (C) Structural requirements, caspase independence, and Bcl-2–mediated inhibition of Vpr-mediated killing. Jurkat cells transfected with the human bcl-2 gene, the neomycin resistance gene only (Neo), or Neo optionally cultured with 50 μM of Z-VAD.fmk were treated with 2 μM Vpr1-96, 2 μM Vpr1-51, 1 μM Vpr52-96 (or mutants), 5 μM Vpr71-96 (or mutants), or 5 μM Vpr83-96, followed by staining with $\Delta\Psi_m$-sensitive $DiOC_6(3)$ (after 2 h as in B), an annexin V–FITC conjugate (for the determination of surface phosphatidylserine exposure, after 12 h of culture), or fixed with ethanol and stained with PI to determine the frequency of hypoploid cells (at 12 h). Data are pooled from five independent experiments, and each data point has been repeated at least three times.

Materials and Methods

Vpr Peptides and Constructs. Vpr1-96, Vpr-derived peptides, and NCp7 where synthetized by automated solid phase synthesis using the FMOC strategy and purified by reverse-phase HPLC (39, 40). The peptides were analyzed by electrospray mass spectrometry and found to be ≥98% pure. The FLAG-Vpr–expressing vector was constructed by PCR amplification of $p90_1$, which contains the whole HIV-1 Lai genome. Both primers, FlVpr (TCCGGATCCACCATGGACTACAAAGACGACGATGACAAATCGATGGAACAAGCCC [coding sequence of the FLAG-derived epitope (MDYKDDDDKS) plus sequence 5,141–5,153 of Lai]) and VLCas (ATTTTCCTATATTCTATGATTACTATGGACC [5,737–5,707]), resulted in a 638-bp fragment, which was cloned into the blunted EcoR1–BamH1 sites of the pcDNA3.1 eukaryotic expression vector (Invitrogen Corp.). This construct was transfected into COS cells using Lipofectamine (Life Technology).

Cells and Apoptosis Modulation. Jurkat-Neo and Jurkat-Bcl-2 clones (reference 41; a gift from Dr. N. Israel, Pasteur Institute, Paris, France), and CEM-C7 cells were cultured in RPMI 1640 Glutamax medium supplemented with 10% FCS, antibiotics, and 0.8 μg/ml G418. 2B4.11 mouse T cell hybridoma cell lines stably transfected with an SFFV.neo vector, containing the human *bcl-2* gene or the neomycin (Neo) resistance gene, and COS cells were cultured in DMEM Glutamax medium supplemented with Hepes, antibiotics, and 10% FCS. PBS-washed cells ($1–5 \times 10^5$/ml) were incubated for 30 min with Vpr or Vpr-derived peptides in isotonic glucose–Hepes buffer (2.4% glucose, 13 mM Hepes, 68 mM NaCl, 1.3 mM KCl, 4 mM Na_2HPO_4, and 0.7 mM KH_2PO_4, pH 7.2), followed by culture in complete culture medium supplemented with cyclosporin A (CsA; 1 μM; Novartis), bongkrekic acid (BA; 50 μM; gift of Dr. J.A. Duine, Delft University, Delft, The Netherlands), and/or the caspase inhibitor *N*-benzyloxycarbonyl-Val-Ala-Asp.fluoromethylketone (Z-VAD.fmk; 50 μM; Bachem Bioscience, Inc.). During exposure to Vpr or Vpr-derived peptides, human primary PBLs from healthy donors, purified with Lymphoprep (Pharmacia), were cultured in RPMI 1640 Glutamax medium without any addition of serum. In contrast, PHA blasts (24 h of 1 μg/ml PHA-P [Wellcome Industries]; 48 h with 100 U/ml human recombinant IL-2 [Boehringer Mannheim]) were cultured with 10% FCS.

Determinations of Apoptosis-associated Alterations in Intact Cells. For cytofluorometry, the following fluorochromes were employed: 3,3′-dihexyloxacarbocyanine iodide ($DiOC_{(6)}3$; 40 nM) for mitochondrial transmembrane potential ($\Delta\Psi_m$) quantification, hydroethidine (4 μM) for the determination of superoxide anion generation, and propidium iodide (PI; 5 μM) for the determination of viability (42). The frequency of subdiploid cells was determined by PI (50 μg/ml) staining of ethanol-permeabilized cells treated with 500 μg/ml RNase (Sigma Chemical Co.; 30 min, room temperature [RT]) in PBS, pH 7.4, supplemented with 5 mM glucose (43). For in situ determinations, cells were fixed with 4% paraformaldehyde and 0.19% picric acid in PBS, pH 7.4, for 1 h at RT. Fixed cells were permeabilized with 0.1% SDS in PBS at RT for 5 min, blocked with 10% FCS, and stained with an mAb specific for native cytochrome *c* (mAb 6H2.B4 [PharMingen], revealed by a goat anti–mouse IgG1 PE conjugate [Southern Biotechnology Associates, Inc.]), Hsp60 (mAb H4149 [Sigma Chemical Co.], revealed by a goat anti–mouse IgG1 FITC conjugate), cytochrome *c* oxidase (COX; mAb 20E8-C12 [Molecular Probes, Inc.], revealed by a goat anti–mouse IgG2a FITC conjugate), or a rabbit antiserum generated against amino acids 151–200 of AIF ([reference 19]; revealed with a goat anti–rabbit IgG conjugated to PE [Southern Biotechnology Associates, Inc.]). Alternatively, unfixed cells were incubated with the $\Delta\Psi_m$-sensitive dyes chloromethyl-X-rosamine (CMXRos; 50 nM; Molecular Probes, Inc.) or 5,5′,6,6′-tetrachloro-1,1′,3,3′-tetraethylbenzimidazolcarbocyanine iodide (JC-1; 1 μM; Molecular Probes, Inc.), the $\Delta\Psi_m$-insensitive dye Mitotracker green (1 μM; Molecular Probes, Inc.), and/or Hoechst 33342 (2 μM; Sigma Chemical Co.) (27). Confocal microscopy was performed on a Leica TC-SP (Leica Microsystems) equipped with an ArKr laser mounted on an inverted Leica DM IFBE microscope with a 63×1.32 NA oil objective.

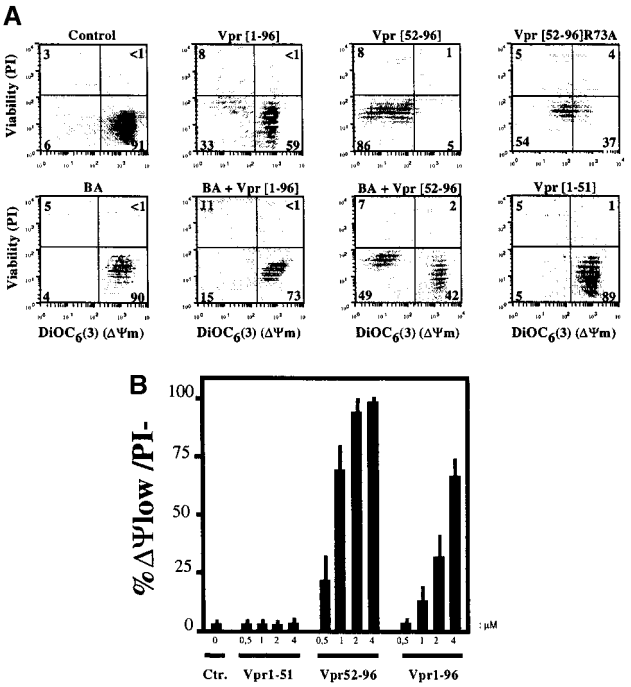

Figure 2. Effects of Vpr on human primary PBLs. (A) Effect of Vpr and Vpr-derived peptides on PBLs. Cells were cultured for 2 h in the presence of 2 μM Vpr, Vpr1-52, Vpr52-96, Vpr52-96R73A, and/or 50 μM BA, followed by staining with PI (for the determination of plasma membrane permeability) and the $\Delta\Psi_m$-sensitive dye $DiOC_6(3)$. (B) Dose–response curve for different Vpr-derived peptides. Results are representative of three independent experiments.

Preparation of Organelles, Cell-free Systems of Apoptosis, and Assessment of Mitochondrial Parameters. Mitochondria were purified from rat liver (36) and resuspended in 250 mM sucrose plus 0.1 mM EGTA plus 10 mM *N*-tris(hydroxymethyl)methyl-2-aminoethanesulfonic acid, pH 7.4. Cytosols from control or αCD95-treated (CH-11; 500 ng/ml; 2 h; Immunotech) cells (10^7 cells/100 μl in cell-free system buffer [reference 37]) were prepared by five freeze–thaw cycles in liquid nitrogen, followed by centrifugation (1.5×10^5 *g*, 4°C, 1 h) as described (37). HeLa cell nuclei (10^3 nuclei per microliter) were incubated (60 min at 37°C) in the presence (or not) of isolated mitochondria, mitochondrial supernatants, cytosols from CEM-C7 cells, or recombinant AIF (19), and/or Vpr peptides. Then, nuclei were stained with PI (10 μg/ml; Sigma Chemical Co.), followed by cytofluorometric determination of the frequency of hypoploid nuclei (37). To determine large amplitude swelling, mitochondria (0.5 mg protein per milliliter) were resuspended in Swelling buffer (200 mM sucrose, 10 mM Tris-MOPS (3-[*N*-morpholino]-propanesulfonic acid), pH 7.4, 5 mM

Tris-succinate, 1 mM Tris-phosphate, 2 μM rotenone, and 10 μM EGTA-Tris) and monitored in an F5400 fluorescence spectrometer (Hitachi) for 90° light scattering (545 nm) after addition of 1 mM atractyloside (Atr; Sigma Chemical Co.), 1 μM CsA, 50 μM BA, and/or Vpr peptides. For determination of $\Delta\Psi_m$, mitochondria (0.5 mg protein per milliliter) were incubated in swelling buffer supplemented with 1 μM rhodamine 123 (Rh123; Molecular Probes, Inc.), and the dequenching of Rh123 fluorescence (excitation 505 nm, emission 525 nm) was measured (44). Supernatants from mitochondria (6,800 *g* for 15 min, then 20,000 *g* for 1 h; 4°C) were frozen at −80°C until determination of AIF activity or immunodetection of cytochrome *c* (mouse mAb clone 7H8.2C12; PharMingen) and AIF (rabbit polyclonal antiserum; reference 19). Caspase activity in the mitochondrial supernatant was measured using Ac-DEVD-amido-4-trifluoromethylcoumarin (Bachem Bioscience, Inc.) as fluorogenic substrate (18).

Binding Assays and Immunoblots. Isolated rat liver mitochondria (250 μg of protein in 100 μl of swelling buffer) were incubated for 30 min at RT with 5 μM Vpr52-96 or biotin–Vpr52-96. The washed mitochondrial pellet (10^4 *g*, 10 min, 4°C; two washes) was then lysed with 150 μl of a buffer containing 20 mM Tris/HCl, pH 7.6, 400 mM NaCl, 50 mM KCl, 1 mM EDTA, 0.2 mM PMSF, aprotinin (100 U/ml), 1% Triton X-100, and 20% glycerol. Such extracts were diluted with two volumes of PBS plus 1 mM EDTA before the addition of 150 μl avidin–agarose (ImmunoPure; Pierce Chemical Co.) to capture the biotin-labeled Vpr52-96 complexed with its mitochondrial ligand(s) (2 h at 4°C in a roller drum). The avidin–agarose was washed batchwise with PBS (five times, 5 ml; 1,000 *g*, 5 min, 4°C), resuspended in 100 μl of twofold-concentrated Laemmli buffer containing 4% SDS and 5 mM β-ME, incubated for 10 min at RT, and centrifuged (1,000 *g*, 10 min, 4°C). Finally, the supernatants were heated at 95°C for 5 min and analyzed by SDS-PAGE (12%), followed by silver staining (BioRad kit) or Western blot and immunodetection of VDAC (antiporin 31HL mAb; Calbiochem Corp.), subunit IV of COX (mAb from Molecular Probes, Inc.), and a rabbit polyclonal antiserum against human ANT (provided by Dr. H.H. Schmid, The Hormel Institute, University of Minnesota, Austin, MN; reference 45). In one series of experiments, PBL-derived PHA lymphoblasts were cultured in the presence of 1 μM biotin–Vpr52-96, followed by fixation/permeabilization (4% paraformaldehyde, 0.19% picric acid in PBS, pH 7.4, for 1 h at RT) and staining with a streptavidin–PE conjugate (Sigma Chemical Co.). For surface plasmon resonance measurements, upgraded Biacore 1000 equipment (Pharmacia) was used. 0.8 ng/mm^2 biotin–Vpr52-96 was absorbed to streptavidin covalently linked to a CMb chip according to the standard procedure. Three dilutions (35, 70, and 140 nM) of ANT (purified to ≥95%, as described above) were passed at a flux of 5 μl/min for 10 min, and data were calculated using BIAeval.3 software (Pharmacia).

Purification and Reconstitution of PTPC, ANT, and Bcl-2/Bax Proteins in Liposomes. PTPC from rat brain or ANT from rat heart was purified and reconstituted into liposomes via detergent dialysis following published protocols (27, 29). Recombinant human Bcl-2 (1-218) or mouse Bax (1-171), both lacking the hydrophobic transmembrane domain and produced and purified as described (25, 27, 29), were added during the dialysis step. Liposomes recovered from dialysis were ultrasonicated, charged on Sephadex G75 or G25 columns (Pharmacia) for PTPC or ANT, respec-

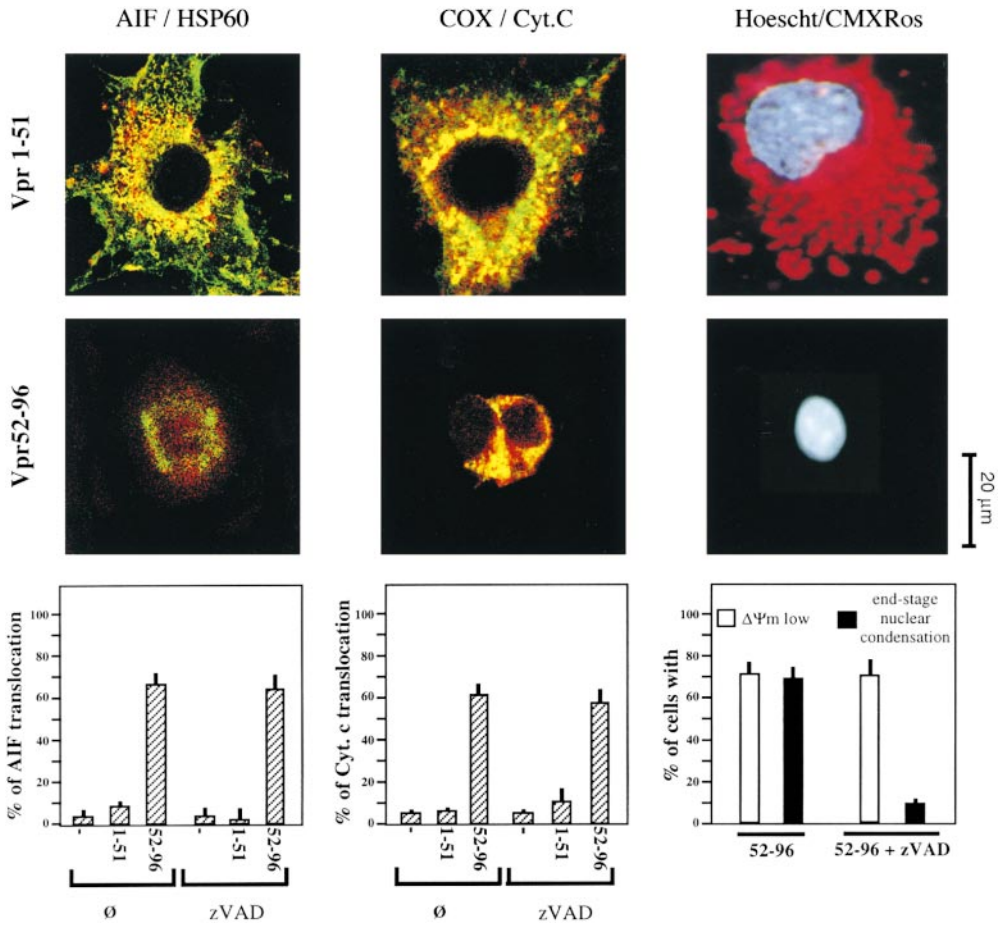

Figure 3. Mitochondrial Vpr effects in intact cells. COS cells were treated for 3 h with 1 μM Vpr1-51 (negative control) or Vpr52-96, fixed, permeabilized, and immunostained with antibodies specific for AIF or cytochrome (Cyt.) *c* (both normally in the mitochondrial intermembrane space revealed PE, red fluorescence) and the mitochondrial matrix protein Hsp60 or the inner mitochondrial membrane protein COX (both revealed by FITC, green fluorescence). In addition, cells were stained with the $\Delta\Psi_m$-sensitive dye CMXRos (red fluorescence) and the DNA intercalating agent Hoechst 33342 (blue fluorescence). The histograms indicate the percentage of cells manifesting mitochondrio-nuclear AIF translocation, mitochondriocytosolic cytochrome *c* translocation, or a low $\Delta\Psi_m$ after treatment with different Vpr peptides (1 μM) in the presence or absence of Z-VAD.fmk (50 μM).

tively, and eluted with 125 mM sucrose plus 10 mM Hepes, pH 7.4. Aliquots ($\sim 10^7$) of liposomes were incubated during 30 min at RT in 125 mM sucrose plus 10 mM Hepes, pH 7.4, in the presence or absence of the indicated Vpr peptides, CsA (1 μM), BA (50 μM), or Atr (50 μM). Then, liposomes were equilibrated with $DiOC_6(3)$ (80 nM, 20–30 min at RT; Molecular Probes, Inc.) and analyzed in a FACSVantage™ cytofluorometer (Becton Dickinson) for $DiOC_6(3)$ retention as described (27, 29). Triplicates of 5×10^4 liposomes were analyzed, and results were expressed as percent reduction of $DiOC_6(3)$ fluorescence, considering the reduction obtained with 0.02% SDS (15 min, RT) as the 100% value.

Yeast Strains and Clonogenic Assays. M3 wild-type *Saccharomyces cerevisiae* (genotype: *MATα lys2 his4 trp1 ade2 leu2 ura3 Can*^{r}); VDACΔ1 (genotype like M3, but VDAC1::LEU2), VDACΔ1Δ2 (genotype like M3, VDAC1::LEU2, VDAC2::TRP1); VDACΔ1,2^{high} (genotype like VDACΔ1, but overexpressing VDAC2 as a multicopy suppressor of low growth phenotype; reference 46); VDACΔ1/hVDAC1 (genotype like VDACΔ1, retransfected with human VDAC; reference 47; gift from Dr. M. Forte, Vollum Institute, Portland, OR). The *S. cerevisiae* W301-1B control strain (*MATα, ade2, leu2, his3, trp1, ura3*), ANTΔ1Δ2 (genotype like W301-1B, but *LEU2::aac1, HIS3::aac2*; reference 48; gift from T. Drgon, National Institutes of Health, Bethesda, MD) and ANTΔ1Δ2 retransfected with the yeast ANT2 gene (reference 49; gift from Dr. M. Klingenberg, University of Munich, Germany) (47, 48) were treated with Vpr-derived peptides (1 h in H_2O) as described (50), followed by plating on standard YPD agarose and quantification of the percentage of surviving clones after 48 h of culture. In addition, PTY44 wild-type yeast cells (genotype: *MATα leu2-3, 112; lys2, trp1-Δ1, ura3-52*) and yme1-Δ1 (genotype like PTY44, but *yme1-Δ1::URA3, TRP1*; gift from K.H. White, University of Wyoming, Laramie, WY; reference 51) were cultured in supplemented DOB medium (Bio 101).

Results and Discussion

Structural Motifs Required for the Cytotoxic Effects of Vpr on Intact Cells. Synthetic Vpr protein (96 amino acids) kills Jurkat lymphoma cells (Fig. 1 A) as well as a variety of other cell lines (references 10 and 11; data not shown). This effect was mimicked by the COOH-terminal moiety of the molecule Vpr52-96 but not by its NH_2-terminal moiety (Vpr1-51; Fig. 1 A). As described for other models of apoptosis (38), Vpr (or Vpr52-96, not Vpr1-51) induced an early loss of $\Delta\Psi_m$, as detected by the potential-sensitive fluorochrome $DiOC_6(3)$ (Fig. 1 B). Abolition of Vpr52-96 homodimerization by replacement of two leucine residues by alanines (L60A L67A; reference 40) did not affect its apoptogenic function. In contrast,

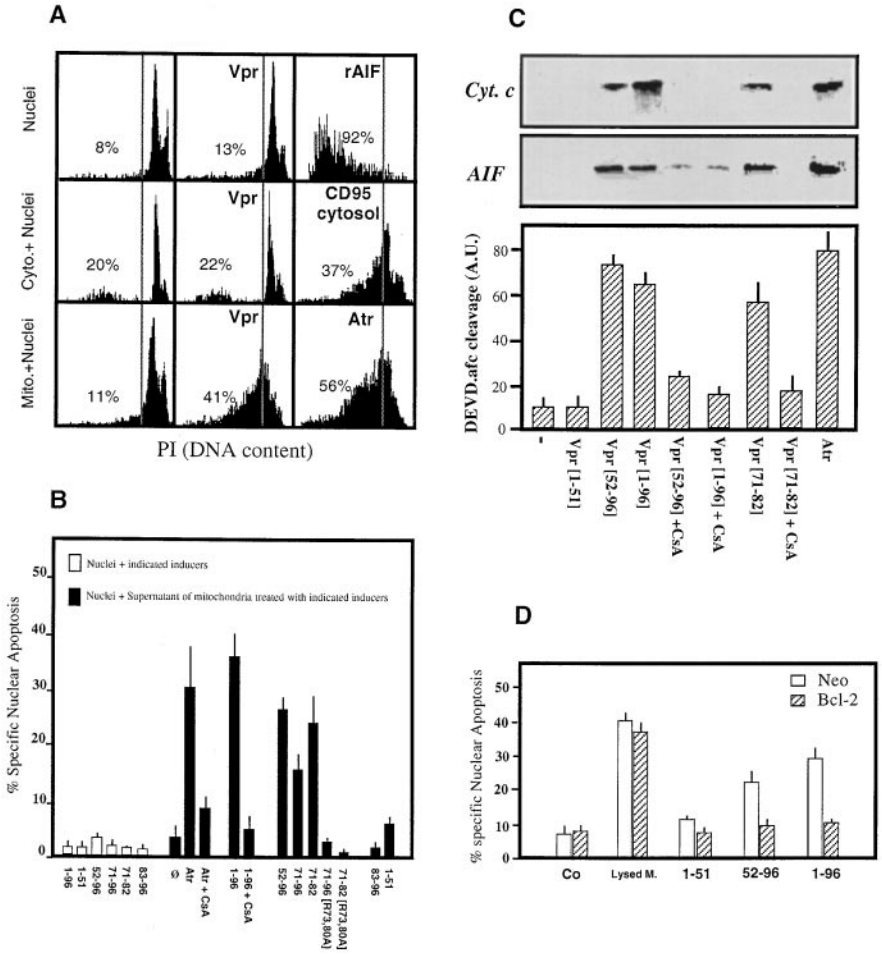

Figure 4. Effects of Vpr on a cell-free system of apoptosis. (A) Determination of the subcellular target of Vpr in a cell-free system of nuclear apoptosis. Nuclei purified from HeLa cells were incubated for 60 min with the indicated combinations of Vpr alone (1 μM), cytosol (Cyto.; obtained from CEM cells/10 μg protein per milliliter), mitochondria (Mito.; purified from mouse liver; 0.5 mg mitochondrial protein per milliliter), recombinant mouse AIF1-612 (100 μg/ml), cytosol from Fas-treated CEM cells (10 μg protein per milliliter), or Atr (1 mM), followed by PI staining and DNA content analysis of nuclei (16). (B) Structural requirements and CsA-mediated inhibition of Vpr-induced release of mitochondrial apoptogenic factors. Mitochondria were treated for 30 min with 1 μM of Vpr or Vpr-derived peptides, 1 μM CsA, and/or 1 mM Atr. The supernatants of these mitochondria were added to purified nuclei for a period of 60 min, followed by PI staining and determination of the frequency of hypoploid nuclei. Alternatively, Vpr-derived peptides were added directly to nuclei. (C) Vpr-induced mitochondrial release of potentially apoptogenic proteins. Mitochondrial supernatants treated as in B were subjected to immunoblot detection of cytochrome (Cyt.) *c* or AIF. Alternatively, the capacity of supernatants to cleave the fluorogenic caspases substrate DEVD.afc was assessed. (D) Bcl-2–mediated inhibition of nuclear apoptosis induced in the cell-free system. Mitochondria (M.) were purified from 2B4.11 T cell hybridoma cells expressing a Neo control vector or human Bcl-2. These organelles were left untreated (Co.), subjected to lysis, or treated with 1 μM of the indicated Vpr-derived peptide, followed by recovery of the supernatant and determination of its apoptogenic effects on isolated HeLa nuclei as in A.

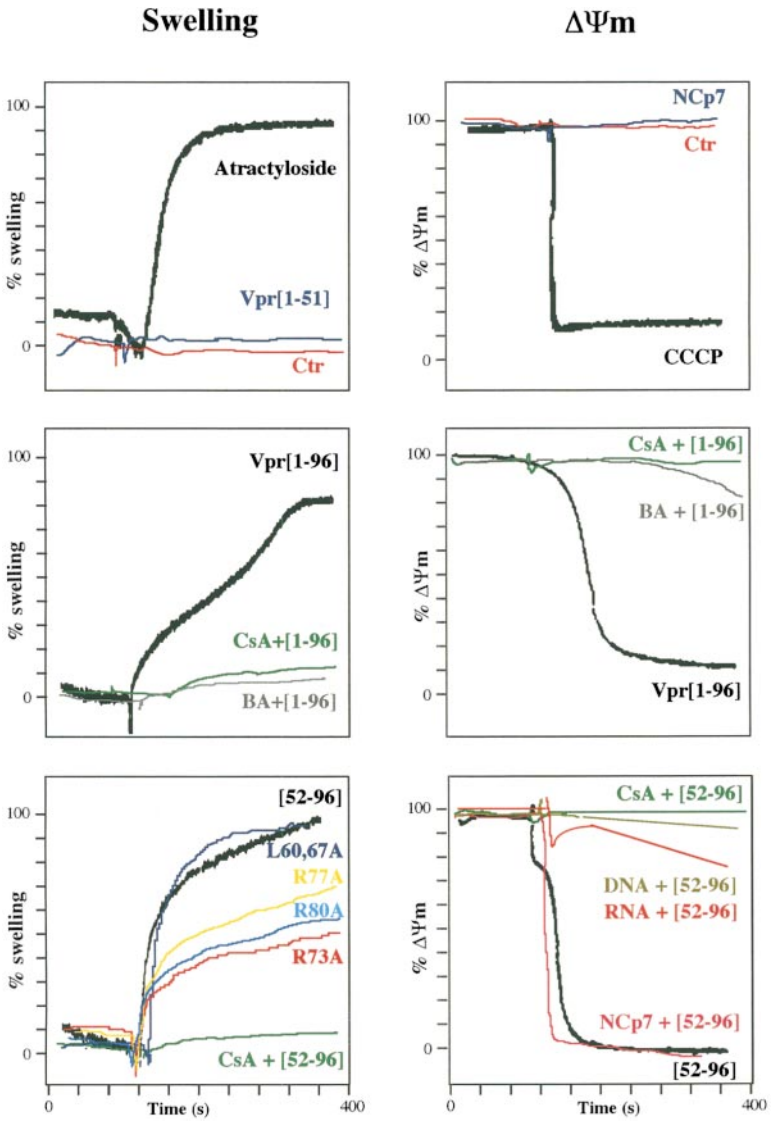

Figure 5. Vpr-induced swelling and $\Delta\Psi_m$ dissipation in isolated mitochondria. Rat liver mitochondria were exposed to Vpr (2 μM) or the indicated Vpr derivative (1 μM), CsA (5 μM; added 1 min before Vpr to mitochondria), BA (50 μM; added 1 min before Vpr to mitochondria), a random eicosadesoxynucleotide (DNA; 1 μM), total cell RNA (1 μM), or Ncp7 (10 μM; added to Vpr 1 min before joint addition to mitochondria). Mitochondrial swelling (measured as 90° light scattering at 545 nm) or the $\Delta\Psi_m$ (measured as Rh123 dequenching) were monitored continuously. $\Delta\Psi_m$ and swelling determinations yielded concordant results. Representative curves obtained with either of the two methods are shown.

replacement of arginine (R) residues situated within or between the two functionally important H(S/F)RIG motifs (52) (R73A or R77A or R80A) greatly reduced the apoptogenic effect of Vpr52-96. A peptide containing this motif (Vpr71-96, but not Vpr71-96 R73A R80A) was sufficient to induce apoptosis (Fig. 1 C). Systematic dose–response studies revealed a significant difference in the ED_{50} of these R-mutated peptides and their wild-type equivalents (see Fig. 6 A). These observations correlate with the fact that R80 mutations reduce cell killing by vesicular stomatitis virus (VSV)-G–pseudotyped HIV-1 in vitro (8) and that R73 and R80 are extremely conserved among pathogenic HIV-1 isolates. Agents that interact with the H(S/F)RIG motifs such as RNA or DNA (53) neutralized the cytocidal effect of Vpr (not shown). A strict correlation was found between the $\Delta\Psi_m$ collapse induced by different Vpr-derived peptides and apoptosis induction at the plasma membrane and nuclear levels (Fig. 1 C). Very similar data have been obtained with several human cell lines (U937, CEM, HeLa), COS cells, and mouse thymocytes (not shown), as well as human primary PBLs (Fig. 2). Thus, Vpr or Vpr52-96 (but not Vpr1-51) causes a $\Delta\Psi_m$ dissipation that precedes the loss of viability in human PBLs, and this effect is reduced when the mutant Vpr52-96 R73A is employed (Fig. 2).

Mitochondrial Effects of Vpr Added to Intact Cells. In Jurkat cells, Vpr caused a loss of $\Delta\Psi_m$, which was followed by an increase in the production of superoxide anion (Fig. 1 B) and nuclear apoptosis (Fig. 1 C). This early effect on the $\Delta\Psi_m$ (1–2 h after addition of Vpr or Vpr52-96) was transiently inhibited by CsA and BA, two inhibitors of the PTPC (Fig. 1 B). Similar results were obtained with primary cells such as mouse thymocytes (not shown) and human primary PBLs, in which the $\Delta\Psi_m$ reducing effect of Vpr or Vpr52-96 is counteracted by the ANT ligand BA (Fig. 2 A). The $\Delta\Psi_m$ loss was also inhibited by overexpression of Bcl-2 (Fig. 1 C), an endogenous cytoprotective protein acting on the PTPC (27, 29). Bcl-2 concomitantly prevented other Vpr-induced features of apoptosis, such as phosphatidylserine exposure on the plasma membrane and nuclear DNA loss (Fig. 1 C). In contrast, the pancaspase inhibitor Z-VAD.fmk

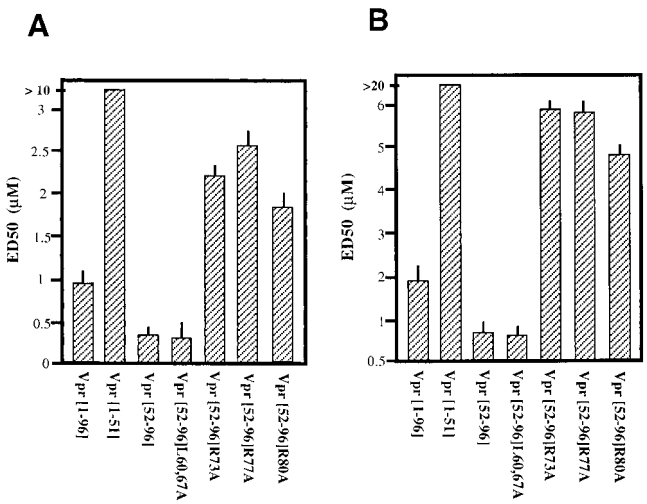

Figure 6. Comparison of the ED_{50} of different Vpr-derived peptides in acute cytotoxicity and mitochondrial swelling assays. (A) Half-maximal effect (ED_{50}) of Vpr-derived peptides on Jurkat cells. Cells were stimulated for 2 h as in Fig. 1 B, followed by cytofluorimetric determination of the frequency of $\Delta\Psi_m^{low}$ cells with $DiOC_6(3)$. The dose causing $\Delta\Psi_m$ dissipation in 50% of the cells was extrapolated as the ED_{50}. Results (X ± SD) were obtained in six independent experiments in which each peptide was tested at least three times. (B) ED_{50} of Vpr-derived peptides on purified mitochondria. Different concentrations of Vpr or Vpr-derived peptides were added to purified mitochondria as in Fig. 5, and the dose yielding an ED_{50} on mitochondrial swelling (measured as 90° light scattering at 545 nm, 300 s after addition of the peptide) was extrapolated from the dose–response curve (log 2 dilutions). Results were obtained in 10 independent experiments, and each peptide was used at least three times.

failed to prevent the $\Delta\Psi_m$ dissipation, although it did reduce the (caspase-dependent) DNA loss resulting in hypoploidy (Fig. 1 C). Vpr52-96 induced, in intact cells, the mitochondrionuclear translocation of AIF and the mitochondriocytosolic translocation of cytochrome *c*, as detected by confocal immunofluorescence microscopy (Fig. 3). Vpr also caused nuclear chromatin condensation (measured with Hoechst 33342), as well as a dissipation of the $\Delta\Psi_m$, as measured with the $\Delta\Psi_m$-sensitive dye CMXRos (Fig. 3). Again, Z-VAD.fmk (which did prevent end-stage nuclear chromatin condensation) had no mitochondrioprotective effects (Fig. 2). Altogether, these findings indicate that the mitochondrial effects of Vpr are caspase independent yet suppressed by PTPC inhibitors such as CsA, BA, or Bcl-2.

Determination of the Subcellular Target Responsible for the Apoptogenic Vpr Effect in a Cell-free System. Vpr has been suggested to act on different subcellular targets including the nucleus (5), the plasma membrane (10, 54), and mitochondria (55). To map the subcellular site of its apoptogenic action, we added Vpr to purified HeLa nuclei and determined the minimum requirements for the induction of chromatin degradation. Vpr alone had no effects on nuclei, nor did it activate any cytosolic activity resulting in nuclear apoptosis (Fig. 4 A). In contrast, Vpr did become apoptogenic in the presence of mitochondria (Fig. 4 A). This suggests that Vpr acts primarily on mitochondria (rather than on nuclei or cytosolic proteins) to trigger the induction of apoptosis. Supernatants of mitochondria treated with Vpr contain a factor that provokes nuclear apoptosis in the cell-free system (Fig. 4 B), immunodetectable AIF (which accounts for this bioactivity; reference 19), immunodetectable cytochrome *c*, and a caspase activity cleaving DEVD.afc (Fig. 4 C) (18, 56). The release of these mitochondrial intermembrane proteins was induced by the entire Vpr molecule, its COOH-terminal moiety (Vpr52-96 or Vpr71-96), or a short peptide fragment containing the two H(S/F)RIG motifs (Vpr71-82) (Fig. 4, B and C), but not by Vpr-derived peptides in which R73 and R80 were mutated (Fig. 4 B). Altogether, the data obtained in the cell-free system suggest that Vpr can exert most if not all of its apoptogenic potential by directly compromising the barrier function of mitochondrial membranes.

Mechanisms of Vpr Effects on Isolated Mitochondria: Structural Analysis and Evidence for the Involvement of the PTPC. The release of mitochondrial proteins induced by Vpr in vitro was blocked by the PT pore inhibitor CsA (Fig. 4, B and C). Moreover, mitochondria isolated from Bcl-2–overexpressing cells were refractory to the Vpr-induced release of AIF activity (Fig. 4 D). The fact that some of the Vpr effects were inhibited by PTPC inhibitors (CsA, BA, or Bcl-2) suggested that Vpr can act on the mitochondrial PT pore, the opening of which can be a rate-limiting step of the apoptotic process. Accordingly, Vpr induced two hallmarks of PTPC opening when added to purified mitochondria, namely mitochondrial volume increase and $\Delta\Psi_m$ dissipation (Fig. 5), and both of these effects were inhibited by CsA and BA. The effect of free holo Vpr on isolated mitochondria is fully mimicked by Vpr52-96 but not by Vpr52-96 R73A, Vpr52-96 R77A, or Vpr52-96 R80A (Fig. 5). Preincubation of Vpr with a molar excess of RNA or DNA (which bind to the Vpr71-82 motif; reference 53) abolished its effects on isolated mitochondria (Fig. 5), correlating with the data obtained in cells (not shown). In contrast, synthetic HIV-1 nucleocapsid protein NCp7 (which binds to the extreme COOH terminus of Vpr; reference 39) does not inhibit Vpr effects on mitochondria (Fig. 5). Thus, the structural motifs of Vpr responsible for direct, presumably PTPC-mediated mitochondrial effects in vitro (Fig. 5) and apoptosis induction in intact cells (Fig. 1 C) are the same. This fact is also underscored by the comparison of the ED_{50} of different Vpr peptides determined on intact cells (Fig. 6 A) and purified mitochondria (Fig. 6 B).

Mitochondrial Localization of Vpr. If Vpr acted on mitochondria to induce apoptosis, then at least some Vpr protein should be found in mitochondria from intact cells. To determine the subcellular localization of Vpr, epitope-tagged (FLAG)Vpr was transfected into COS cells and was revealed by a PE-labeled anti-FLAG antibody (red fluorescence). Simultaneously, mitochondria were stained with an FITC-conjugated anti-Hsp60 antibody (green fluorescence). In accord with previous observations of a punctuate cytoplasmic localization of Vpr (57, 58), we found that ~30% of Vpr-expressing cells exhibited an exclusively cytoplasmic Vpr staining pattern (Fig. 7 A). These cells appear to be programmed to die (not shown), which may explain why they represent only a fraction of the entire population. In such cells, most of the Vpr-dependent red fluorescence colo-

calizes with the Hsp60 protein, giving rise to a yellow (red plus green) staining pattern. Very little Vpr is localized in the nonmitochondrial compartment (red fluorescence; Fig. 7 A). To confirm this observation in another experimental system, we added biotinylated Vpr52-96 to human primary PBLs or to PHA lymphoblasts. Vpr52-96 was then detected by means of a streptavidin–PE conjugate. Cells were counterstained with Mitotracker green (which labels mitochondria independently from their $\Delta\Psi_m$) and Hoechst 33342 (which labels nuclei) to determine the subcellular distribution of Vpr. After an initial enrichment in the plasma membrane (not shown), biotinylated Vpr52-96 was specifically recruited to mitochondria (Fig. 7 B).

Direct Interaction of Vpr with the PTPC via ANT. To identify the putative mitochondrial receptor of Vpr, purified mitochondria were incubated with biotinylated Vpr52-96 (which is as efficient as nonmodified Vpr52-96 in inducing mitochondrial swelling; not shown), followed by purification of biotin–Vpr52-96 binding proteins on avidin–agarose. This led to the selective recovery of very few proteins, among which we identified VDAC and ANT (but not COX) by immunoblotting (Fig. 8 A). Neither VDAC nor ANT was recovered if mitochondria were pretreated with BA (Fig. 8 B), indicating that BA can compete with Vpr52-96 for ANT binding and/or that a BA-induced conformational change abolishes the Vpr–ANT interaction. Surface plasmon resonance (see Materials and Methods) measurements confirmed that biotinylated Vpr52-96 immobilized to a streptavidin matrix binds to purified (>95%) ANT with an affinity constant of $K_A = 7.4 \times 10^8\ M^{-1}$ ($k_{on} = 1.61 \times 10^6\ M^{-1}s^{-1}$; $k_{off} = 2.16 \times 10^{-3}\ s^{-1}$). These results suggest that Vpr is recruited to the PTPC via a direct, specific interaction with ANT.

To confirm the hypothesis that Vpr might permeabilize mitochondrial membranes by a direct effect on the PTPC, we purified this molecular complex from brain (27, 29), reconstituted it into liposomes, and measured the capacity of Vpr to permeabilize the liposomal membrane (Fig. 9 A). Vpr or Vpr52-96 increases the permeability of liposomes containing the PTPC, and this effect is inhibited by CsA or BA (Fig. 9 A). In addition, Vpr52-96 acts on a combination of two proteins from the PTPC, ANT plus Bax, and this effect is suppressed by recombinant Bcl-2 (Fig. 9 B). Thus, Vpr acts on the PTPC to perturb the barrier function of mitochondrial membranes.

Genetic Evidence for PTPC-mediated Vpr Cytotoxicity. The essential components of the PTPC include the two most abundant proteins of the outer and inner mitochondrial membranes, VDAC and ANT, respectively (27, 29, 30). We therefore examined the cytotoxic effect of Vpr52-96 on a series

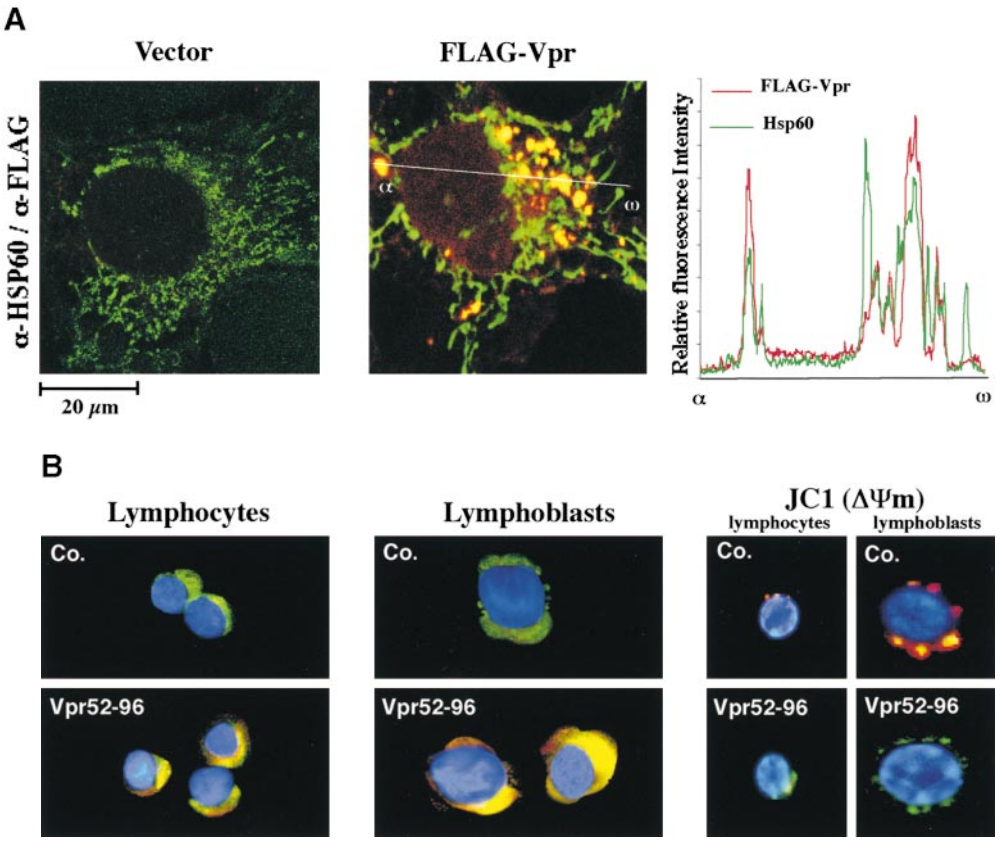

Figure 7. Subcellular localization of Vpr in different cell types. (A) Subcellular localization of transfected Vpr. COS cells were transfected with pcDNA3.1 vector only or with pcDNA-FLAG-Vpr expression vector, followed by immunofluorescence detection (mouse mAb M2 anti-FLAG; Sigma Chemical Co.) of the FLAG (red fluorescence) as well as of the mitochondrial protein Hsp60 (green fluorescence) by confocal microscopy. Fine analysis of the fluorescence distribution (right panel) reveals partial colocalization of Vpr and Hsp60. The micrograph of the FLAG-Vpr–expressing cells represents ~30% of the transfected cells with a predominantly cytoplasmic staining. The remaining cells showed either a predominantly nuclear/perinuclear Vpr (~40%) distribution or a mixed (~20%) phenotype. (B) Subcellular localization of soluble Vpr52-96 added to cells. Primary human PBLs or PHA lymphoblasts derived from them were incubated in the absence (Co.) or presence of 1 μM biotin–Vpr52-96 for 30 min, counterstained with Mitotracker green (100 nM during the last 30 min of culture), fixed, and stained with a streptavidin–PE conjugate (red fluorescence) as well as the DNA intercalating dye Hoechst 33324 (blue fluorescence). Note the clear overlap between green and red fluorescence (yellow), indicating a mitochondrial localization of Vpr52-96 30 min after the addition of the peptide. Aliquots from control cells and biotin–Vpr52-96–treated cells were stained with the potential-sensitive dye JC-1 (right panel). Control cells exhibited an elevated $\Delta\Psi_m$ (red fluorescence), whereas Vpr52-96–treated cells had a low $\Delta\Psi_m$ (green fluorescence). Micrographs are representative for >90% of the cells, and the experiment was performed four times.

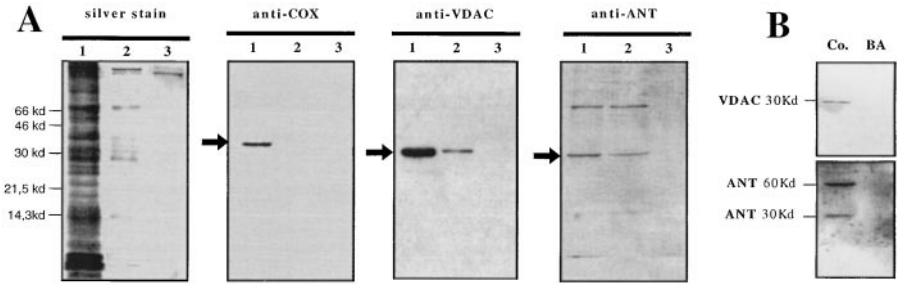

Figure 8. Vpr interaction with the PTPC. (A) Retention of ANT and VDAC by Vpr. Rat liver mitochondria were incubated with buffer only (lane 1), NH_2-terminally biotinylated Vpr52-96 (lane 2), or nonbiotinylated Vpr52-96 (lane 3), followed by triton solubilization and purification of proteins interacting with Vpr–biotin–avidin–agarose complex. As a control, the whole mitochondrial lysate (lane 1) or the avidin-recovered proteins (lanes 2 and 3) were separated by agarose gel electrophoresis, followed by silver staining or immunodetection of COX (subunit IV; 37 kD), VDAC (32 kD), and ANT (30 kD and dimer of 60 kD). Arrows indicate specific bands of the expected molecular size. (B) Inhibition of ANT and VDAC binding to Vpr by BA. Rat liver mitochondria were preincubated for 10 min in the absence (Co.) or presence of 50 μM BA, followed by purification of proteins interacting with biotinylated Vpr52-96 as in A. Then, ANT or VDAC were detected as in A.

of *S. cerevisiae* (yeast) strains in which VDAC or ANT had been invalidated by homologous recombination. Yeast cells rendered deficient for one or two of the principal VDAC isoforms (VDACΔ1 or VDACΔ1Δ2) or the two principal ANT isoforms (ANTΔ1Δ2) are more resistant to Vpr52-96 than their respective wild-type control cells (Fig. 10, A and B). This relative resistance is abolished by genetic interventions known to correct the metabolic deficiencies caused by VDAC1 knockout (overexpression of VDAC2 or transfection with human VDAC1; references 46 and 47; Fig. 10 B) or ANT1/2 knockout (retransfection with yeast ANT2; references 48 and 49; Fig. 10 A). Thus, genetic manipulations confirm that PTPC components are rate limiting for the cytotoxic effect of Vpr.

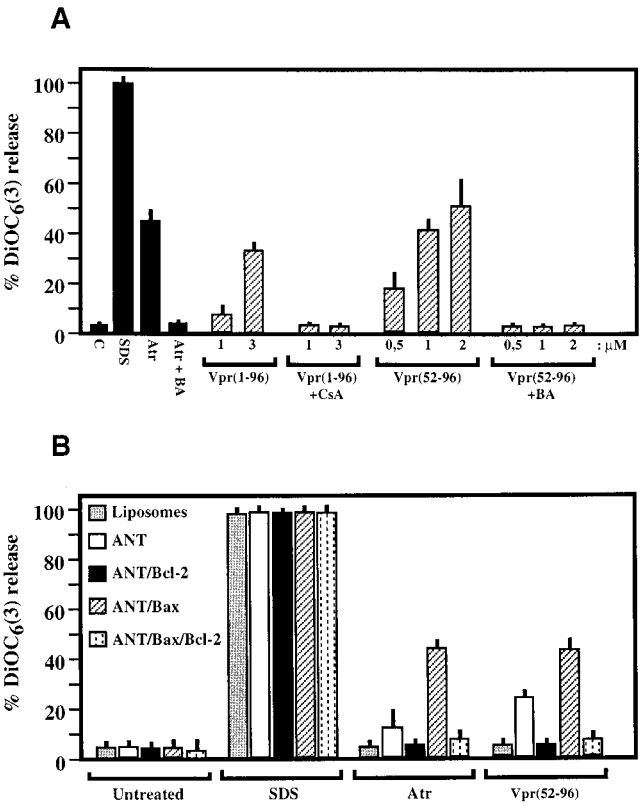

Figure 9. Effects of Vpr on the PTPC or PTPC components reconstituted into liposomes. (A) Effect of Vpr on purified PTPCs. PTPCs were reconstituted into phosphatidylcholine/cholesterol liposomes (26). These PTPC liposomes were loaded with $DiOC_6(3)$, the retention of which was measured after treatment with SDS (0.1%), Atr (250 μM), or the indicated Vpr peptides ± BA (50 μM) or CsA (1μM), as detailed in Materials and Methods. (B) Effect of Vpr on liposomes containing purified individual proteins. Phosphatidylcholine/cardiolipin liposomes containing ANT (from rat heart), Bcl-2 (recombinant), and/or Bax (recombinant) at a molar ratio of 4:4:1 were treated with SDS (0.1%), Atr (100 μM), or Vpr52-96 (1 μM), followed by determination of $DiOC_6(3)$ release. Data are representative of three independent experiments.

Conclusion. Based on the evidence obtained with cells (Figs. 1–3, 6 A, and 7), cell-free systems of apoptosis (Fig. 4), isolated mitochondria (Fig. 5 and Fig. 6 B), purified PTPC (Fig. 9 A), purified ANT and Bax (Fig. 9 B) and VDAC/ANT-deficient yeast cells (Fig. 10), it appears that the acute apoptogenic effect of Vpr involves a direct effect on the PTPC. This conclusion is corroborated by the interaction of Vpr with mitochondria (Fig. 7), with proteins from the PTPC (Fig. 8 and Fig. 9 A), and in particular with the ANT (Fig. 9 B and surface plasmon resonance data). Additional mechanisms of Vpr-mediated apoptosis induction have been suggested, in particular a glucocorticoid-like effect on T cells (11), plasma membrane permeabilization in neurons (10, 54) (which would, however, involve the NH_2 terminus of Vpr, not the COOH terminus), and cell cycle arrest in proliferating cells (5, 7, 9). Thus, the mechanisms of cell killing by Vpr may be redundant, at least in some systems. However, data supporting mitochondrial Vpr effects have been obtained with different cells (Jurkat, CEM, U937, COS, Rat-1, thymocytes, and human primary PBLs; Figs. 1–3, Fig. 7, and data not shown), purified mitochondria from distinct organs (lymphocytes and liver; Figs. 4 and 5), PTPC from brain (Fig. 9 A), and a xenogenic yeast system (Fig. 10), underlining the relative importance of this pathway for Vpr-mediated cell killing.

Vpr and its COOH-terminal moiety have acute cytotoxic (2 h) and mitochondriotoxic (5 min) effects at an ED_{50} of ~1 μM, which is higher than the Vpr serum concentration. This might be used as an argument against the pathophysiological relevance of our studies. Nevertheless, several considerations have to be taken into account. First, the mitochondrial receptor for Vpr, the ANT, possesses a K_a of $7.4 \times 10^{-8}\ M^{-1}$, meaning that chronic exposure to Vpr may well have biological effects at lower doses than those required in short-term assays (in which Vpr must cross several diffusion barriers to reach its target). Accordingly, the

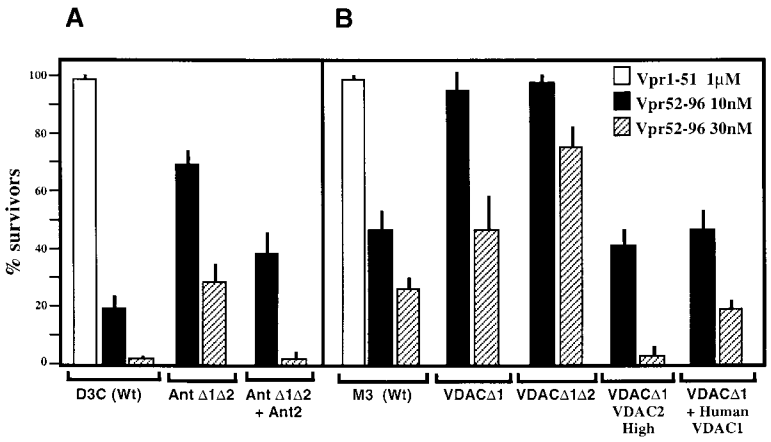

Figure 10. Effect of Vpr-derived peptides on the clonogenic survival of yeast cells deficient for ANT (A) or VDAC (B). The indicated yeast strains were treated with the indicated doses of Vpr52-96 or Vpr1-51, followed by plating on standard YPD agarose and determination of the percentage of surviving clones. This experiment was performed twice, yielding similar results. Vpr was as toxic for a yeast strain lacking the mitochondrial chaperone/protease YME1 as for its wild-type control (not shown), thus excluding that respiratory deficiency causes Vpr resistance in a nonspecific fashion (not shown).

ED_{50} of Vpr52-96 was found to be ~120 nM if cytotoxic effects were assessed after 24 h (not shown); that is at least three times lower than the ED_{50} measured after 2 h (Fig. 6 A). Second, compartmentalization effects might give rise to locally elevated concentrations, which suffice to exert biological effects in situ. Third, when cooperating with other cytotoxic mechanisms, in the context of viral infection, Vpr might exert its effects at lower doses. Two other HIV-1 proteins, Tat and PR, may indirectly affect mitochondrial function, Tat via downregulating mitochondrial superoxide dismutase (59) and PR by cleaving Bcl-2 (60). This hints at the possibility that several apoptogenic HIV-1 proteins—Vpr, Tat, and PR—cooperate at the mitochondrial level, thereby explaining that a fraction of circulating and sessile lymphocytes from HIV-1 carriers have a low $\Delta\Psi_m$ (61, 62).

At the time of this writing, the extent to which Vpr contributes to HIV-1–induced apoptosis in infected or bystander cells is elusive. Early during replication, most if not all Vpr (which is of viral origin) is found in the preintegration complex, where it interacts with nucleic acids (which inhibit the mitochondrial effects of Vpr; Fig. 5) and NCp7, as well as other proteins (63). Moreover, during the later stage of the viral life cycle, Vpr synthesized de novo by the host cell may be sequestered into viral particles before it interacts with its mitochondrial receptor. Alternatively, Vpr may be released and then act on noninfected bystander cells. In vitro, HIV-1 strains in which endogenous Env has been replaced by the general fusogene VSV-G can infect most mammalian cell types yet induce apoptosis in a largely Vpr-dependent fashion (9). Thus, at least in some particular settings, Vpr is rate limiting for HIV-1–mediated killing. It is not known, however, whether this effect is mediated by Vpr produced by the infected cells or rather involves paracrine effects. However, the fact that such Vpr-dependent killing can be obtained in the absence of HIV-1 replication (64) underlines the possibility that virion-associated Vpr (as opposed to free soluble Vpr) may well have a cytocidal potential at the beginning of the viral life cycle.

Viruses employ several strategies for the inhibition of apoptosis. Thus, viruses may encode homologues of mammalian Bcl-2, FLIP (FLICE-inhibitory protein), inhibitor of apoptosis proteins (IAPs), or caspase inhibitors to prevent apoptosis induction during their replication (65). In addition, many viruses induce apoptosis at the end of the replication cycle, perhaps as a strategy to hijack the phagocyte system or to disseminate virions to neighboring cells. To our knowledge, Vpr from HIV-1 constitutes the first example of an apoptogenic viral protein acting on the PTPC. It is tempting to speculate that similar endogenous peptides may exist in animal cells and may link proapoptotic signaling to mitochondrial membrane permeabilization. Such peptides are actually known. They include proapoptotic members of the Bcl-2/Bax family (24–27), as well as the proapoptotic peptides from *Drosophila melanogaster*, Hid, Reaper, and Grim, all of which have recently been shown to act on and/or physically interact with mitochondria (66–68). The NMR structure of the Vpr domain critical for its mitochondrial effects (71HFRIGCRHSRIG82) has been elucidated within Vpr52-96 (40). It is a helical peptide with three positively charged R residues clustered on one side of the helix (40). Substitution of these residues abolishes the apotogenic potential of Vpr (Fig. 1 and Figs. 3–6), underlining their importance for Vpr-mediated killing. However, primary sequence comparisons with Bax, Bak, Bid, Hid, Reaper, or Grim do not reveal any obvious homology between these proteins and Vpr. Future studies will unravel whether motifs resembling the mitochondrio/cytotoxic domain of Vpr can be identified in such proteins or yet to be discovered mammalian Vpr analogues.

Irrespective of these theoretical considerations, this report establishes that Vpr is a novel viral effector that directly targets the PTPC to permeabilize mitochondrial membranes and induce apoptosis. Based on the premise that the PTPC exists in all cell types, Vpr thus exploits a general mechanism to exert its broad cytocidal activity.

We thank Drs. T. Drgon, M. Forte, N. Israel, M. Klingenberg, D. Piatier-Tonneau, D. Rebouillat, H.H. Schmid, X. Sitthy, and K.H. White for the generous gift of reagents and Nathanael Larochette (Centre National de la Recherche Scientifique [CNRS], Villejuif, France) for technical assistance. Our acknowledgments to Dr. L. Edelman (Institut Pasteur) for advice and continual help.

This work has been supported by grants from Agence Nationale pour le Recherche contre le SIDA, Association pour la Recherche sur le Cancer, CNRS, Fondation pour la Recherche Médicale, IN-

SERM, Ligue Nationale contre le Cancer, French Ministry for Science, and Sidaction (to G. Kroemer). E. Jacotot receives a fellowship from Sidaction, L. Ravagnan from the French Ministry of Science, and H.L.A. Vieira from the Portuguese Government (Fundaçäo par a Ciência e Tecnologia, PRAXIS XXI).

Submitted: 9 June 1999
Revised: 12 October 1999
Accepted: 15 October 1999

References

1. Levy, J.A. 1993. Pathogenesis of HIV infection. *Microbiol. Rev*. 57:222–230.
2. Fauci, A.S. 1996. Host factors and the pathogenesis of HIV-induced disease. *Nature*. 384:529–534.
3. Emerman, M., and M.H. Malim. 1998. HIV-1 regulatory/accessory genes: keys to unraveling viral and host cell biology. *Science*. 280:1880–1884.
4. Hellerstein, M., M.B. Hanley, D. Cesar, C. Papageorgopoulos, E. Wieder, D. Schmidt, R. Hoh, R. Neese, D. Macallan, S. Deeks, et al. 1999. Directly measured kinetics of circulating T lymphocytes in normal and HIV-1-infected humans. *Nat. Med*. 5:83–89.
5. Cullen, B.R. 1998. HIV-1 auxiliary proteins: making connections in a dying cell. *Cell*. 93:685–692.
6. Levy, D.N., Y. Refaeli, B.R. MacGregor, and D.B. Weiner. 1994. Serum Vpr regulates productive infection and latency of human immunodeficiency virus type 1. *Proc. Natl. Acad. Sci. USA*. 91:10873–10877.
7. Goh, W.C., M.E. Rogel, C.M. Kinsey, S.F. Michale, P.N. Fultz, M.A. Nowak, B.H. Hahn, and M. Emerman. 1998. HIV-1 Vpr increases viral expression by manipulation of the cell cycle: a mechanism for selection of Vpr in vivo. *Nat. Med*. 4:65–71.
8. Yao, X.J., A.J. Mouland, R.A. Subbramanian, J. Forget, N. Rougeau, D. Bergeron, and E.A. Cohen. 1998. Vpr stimulates viral expression and induces cell killing in human immunodeficiency virus type 1-infected dividing Jurkat T cells. *J. Virol*. 72:4686–4693.
9. Stewart, S.A., B. Poon, J.B.M. Jowett, and I.S.Y. Chen. 1997. Human immunodeficiency virus type 1 vpr induces apoptosis following cell cycle arrest. *J. Virol*. 71:5579–5592.
10. Piller, S.C., P. Jans, P.W. Gage, and D.A. Jans. 1998. Extracellular HIV-1 virus protein R causes a large inward current and cell death in cultured hippocampal neurons: implications for AIDS pathology. *Proc. Natl. Acad. Sci. USA*. 95:4595–4600.
11. Ayyavoo, V., A. Mahboubi, S. Mahalingam, R. Romalingam, S. Kudchodkar, W.V. Williams, D.R. Green, and D.B. Weiner. 1997. HIV-1 Vpr suppresses immune activation and apoptosis through regulation of nuclear factor kappa B. *Nat. Med*. 10:1117–1123.
12. Lazebnik, Y.A., S. Cole, C.A. Cooke, W.G. Nelson, and W.C. Earnshaw. 1993. Nuclear events of apoptosis in vitro in cell-free mitotic extracts: a model system for analysis of the active phase of apoptosis. *J. Cell Biol*. 123:7–22.
13. Zamzami, N., S.A. Susin, P. Marchetti, T. Hirsch, I. Gómez-Monterrey, M. Castedo, and G. Kroemer. 1996. Mitochondrial control of nuclear apoptosis. *J. Exp. Med*. 183:1533–1544.
14. Liu, X.S., C.N. Kim, J. Yang, R. Jemmerson, and X. Wang. 1996. Induction of apoptotic program in cell-free extracts: requirement for dATP and cytochrome C. *Cell*. 86:147–157.
15. Susin, S.A., N. Zamzami, M. Castedo, T. Hirsch, P. Marchetti, A. Macho, E. Daugas, M. Geuskens, and G. Kroemer. 1996. Bcl-2 inhibits the mitochondrial release of an apoptogenic protease. *J. Exp. Med*. 184:1331–1342.
16. Ellerby, H.M., S.J. Martin, L.M. Ellerby, S.S. Naiem, S. Rabizadeh, G.S. Salvesen, C.A. Casiano, N.R. Cashman, D.R. Green, and D.E. Bredesen. 1997. Establishment of a cell-free system of neuronal apoptosis: comparison of premitochondrial, mitochondrial, and postmitochondrial phases. *J. Neurosci*. 17:6165–6178.
17. Kluck, R.M., E. Bossy-Wetzel, D.R. Green, and D.D. Newmeyer. 1997. The release of cytochrome c from mitochondria: a primary site for Bcl-2 regulation of apoptosis. *Science*. 275:1132–1136.
18. Susin, S.A., H.K. Lorenzo, N. Zamzami, I. Marzo, N. Larochette, P.M. Alzari, and G. Kroemer. 1999. Mitochondrial release of caspases-2 and -9 during the apoptotic process. *J. Exp. Med*. 189:381–394.
19. Susin, S.A., H.K. Lorenzo, N. Zamzami, I. Marzo, B.E. Snow, G.M. Brothers, J. Mangion, E. Jacotot, P. Costantini, M. Loeffler, et al. 1999. Molecular characterization of mitochondrial apoptosis-inducing factor (AIF). *Nature*. 397:441–446.
20. Liu, X.S., P. Li, P. Widlack, H. Zou, X. Luo, W.T. Garrard, and X.D. Wang. 1998. The 40-kDa subunit of DNA fragmentation factor induces DNA fragmentation and chromatin condensation during apoptosis. *Proc. Natl. Acad. Sci. USA*. 95:8461–8466.
21. Enari, M., H. Sakahira, H. Yokoyoma, K. Okawa, A. Iwamtsu, and S. Nagata. 1998. A caspase-activated DNase that degrades DNA during apoptosis, and its inhibitor ICAD. *Nature*. 391:43–50.
22. Samali, A., J. Cai, B. Zhivotovsky, D.P. Jones, and S. Orrenius. 1999. Presence of a pre-apoptotic complex of procaspase-3, hsp60, and hsp10 in the mitochondrial fraction of Jurkat cells. *EMBO (Eur. Mol. Biol. Organ.) J*. 18:2040–2048.
23. Xanthoudakis, S., S. Roy, D. Rasper, T. Hennessey, Y. Aubin, R. Cassady, P. Tawa, R. Ruel, A. Rosen, and D.W. Nicholson. 1999. Hsp60 accelerates the maturation of procaspase-3 by upstream activator proteases during apoptosis. *EMBO (Eur. Mol. Biol. Organ.) J*. 18:2049–2056.
24. Cosulich, S.C., V. Worrall, P.J. Hege, S. Green, and P.R. Clarke. 1997. Regulation of apoptosis by BH3 domains in a cell-free system. *Curr. Biol*. 12:913–920.
25. Jürgensmeier, J.M., Z. Xie, Q. Deveraux, L. Ellerby, D. Bredesen, and J.C. Reed. 1998. Bax directly induces release of cytochrome c from isolated mitochondria. *Proc. Natl. Acad. Sci. USA*. 95:4997–5002.
26. Luo, X., I. Budiharjo, H. Zou, C. Slaughter, and X. Wang. 1998. Bid, a Bcl-2 interacting protein, mediates cytochrome c release from mitochondria in response to activation of cell surface death receptors. *Cell*. 94:481–490.
27. Marzo, I., C. Brenner, N. Zamzami, J. Jürgensmeier, S.A. Susin, H.L.A. Vieira, M.-C. Prévost, Z. Xie, S. Matsuyama, J.C. Reed, et al. 1998. Bax and adenine nucleotide translocator cooperate in the mitochondrial control of apoptosis. *Science*. 281:2027–2031.
28. Narita, M., S. Shimizu, T. Ito, T. Chittenden, R.J. Lutz, H. Matsuda, and Y. Tsujimoto. 1998. Bax interacts with the permeability transition pore to induce permeability transition and cytochrome c release in isolated mitochondria. *Proc. Natl. Acad. Sci. USA*. 95:14681–14686.
29. Marzo, I., C. Brenner, N. Zamzami, S.A. Susin, G. Beutner, D. Brdiczka, R. Rémy, Z.-H. Xie, J.C. Reed, and G. Kroemer. 1998. The permeability transition pore complex: a target for apoptosis regulation by caspases and Bcl-2 related pro-

teins. *J. Exp. Med.* 187:1261–1271.
30. Crompton, M., S. Virji, and J.M. Ward. 1998. Cyclophilin-D binds strongly to complexes of the voltage-dependent anion channel and the adenine nucleotide translocase to form the permeability transition pore. *Eur. J. Biochem.* 258:729–735.
31. Ravagnan, L., I. Marzo, P. Costantini, S.A. Susin, N. Zamzami, P.X. Petit, F. Hirsch, M.-F. Poupon, L. Miccoli, Z. Xie, et al. 1999. Lonidamine triggers apoptosis via a direct, Bcl-2-inhibited effect on the mitochondrial permeability transition pore. *Oncogene*. 18:2537–2546.
32. Fulda, S., C. Scaffidi, S.A. Susin, P.H. Krammer, G. Kroemer, M.E. Peter, and K.M. Debatin. 1998. Activation of mitochondria and release of mitochondrial apoptogenic factors by betulinic acid. *J. Biol. Chem.* 273:33942–33948.
33. Larochette, N., D. Decaudin, E. Jacotot, C. Brenner, I. Marzo, S.A. Susin, N. Zamzami, Z. Xie, J.C. Reed, and G. Kroemer. 1999. Arsenite induces apoptosis via a direct effect on the mitochondrial permeability transition pore. *Exp. Cell Res.* 249:413–421.
34. Zamzami, N., I. Marzo, S.A. Susin, C. Brenner, N. Larochette, P. Marchetti, J. Reed, R. Kofler, and G. Kroemer. 1998. The thiol-crosslinking agent diamide overcomes the apoptosis-inhibitory effect of Bcl-2 by enforcing mitochondrial permeability transition. *Oncogene*. 16:1055–1063.
35. Trost, L.C., and J.J. Lemasters. 1996. The mitochondrial permeability transition: a new pathophysiological mechanism for Reye's syndrome and toxic liver injury. *J. Pharmacol. Exp. Ther.* 278:1000–1005.
36. Costantini, P., B.V. Chernyak, V. Petronilli, and P. Bernardi. 1996. Modulation of the mitochondrial permeability transition pore by pyridine nucleotides and dithiol oxidation at two separate sites. *J. Biol. Chem.* 271:6746–6751.
37. Susin, S.A., N. Zamzami, M. Castedo, E. Daugas, H.-G. Wang, S. Geley, F. Fassy, J. Reed, and G. Kroemer. 1997. The central executioner of apoptosis. Multiple links between protease activation and mitochondria in Fas/Apo-1/CD95- and ceramide-induced apoptosis. *J. Exp. Med.* 186:25–37.
38. Kroemer, G., B. Dallaporta, and M. Resche-Rigon. 1998. The mitochondrial death/life regulator in apoptosis and necrosis. *Annu. Rev. Physiol.* 60:619–642.
39. De Rocquigny, H., P. Petit-Jean, V. Tanchou, D. Decimo, L. Drouot, T. Delaunay, J.L. Darlix, and B.P. Roques. 1997. The zinc fingers of HIV nucleocapsid protein NCp7 direct interactions with the viral regulatory protein Vpr. *J. Biol. Chem.* 272:30753–30759.
40. Schüler, W., K. Wecker, H. de Rocquigny, Y. Baudat, J. Sire, and B.P. Roques. 1999. NMR structure of the (52-96) C-terminal domain of the HIV-1 regulatory protein Vpr: molecular insights into its biological functions. *J. Mol. Biol.* 285:2105–2117.
41. Aillet, F., H. Masutani, C. Elbim, H. Raoul, L. Chene, M.T. Nugeyre, C. Paya, F. Barre-Sinoussi, M.A. Gougerot-Pocidalo, and N. Israel. 1998. Human immunodeficiency virus induces a dual regulation of Bcl-2, resulting in persistent infection of $CD4^+$ T- or monocytic cell lines. *J. Virol.* 72:9698–9705.
42. Zamzami, N., P. Marchetti, M. Castedo, D. Decaudin, A. Macho, T. Hirsch, S.A. Susin, P.X. Petit, B. Mignotte, and G. Kroemer. 1995. Sequential reduction of mitochondrial transmembrane potential and generation of reactive oxygen species in early programmed cell death. *J. Exp. Med.* 182: 367–377.
43. Nicoletti, I., G. Migliorati, M.C. Pagliacci, and C. Riccardi. 1991. A rapid simple method for measuring thymocyte apoptosis by propidium iodide staining and flow cytometry. *J. Immunol. Methods.* 139:271–280.
44. Shimizu, S., Y. Eguchi, W. Kamiike, Y. Funahashi, A. Mignon, V. Lacronique, H. Matsuda, and Y. Tsujimoto. 1998. Bcl-2 prevents apoptotic mitochondrial dysfunction by regulating proton flux. *Proc. Natl. Acad. Sci. USA*. 95:1455–1459.
45. Giron-Calle, J., and H.H. Schmid. 1996. Peroxidative modification of a membrane protein. Conformation-dependent chemical modification of adenine nucleotide translocase in Cu^{2+}/tert-butylhydroperoxide treated mitochondria. *Biochemistry*. 35:15440–15446.
46. Blachly-Dyson, E., J.M. Song, W.J. Wolgang, M. Colombini, and M. Forte. 1997. Multicopy suppressors of phenotypes resulting from the absence of yeast VDAC encode a VDAC-like protein. *Mol. Cell. Biol.* 17:5727–5738.
47. Blachly-Dyson, E., E.B. Zambronicz, W.H. Yu, V. Adams, E.R. McCabe, J. Adelman, M. Colombini, and M. Forte. 1993. Cloning and functional expression in yeast of two human isoforms of the outer mitochondrial membrane channel, the voltage dependent anion channel. *J. Biol. Chem.* 268: 1835–1841.
48. Drgon, T., L. Sabova, N. Nelson, and J. Kolarov. 1991. ADP/ATP translocator is essential for anaerobic growth of yeast *Saccharomyces cerevisiae*. *FEBS Lett.* 289:159–162.
49. Nelson, D.R., J.E. Lawson, M. Klingenberg, and M.G. Douglas. 1993. Site-directed mutagenesis of the yeast mitochondrial ADP/ATP translocator-6 arginines and one lysine are essential. *J. Mol. Biol.* 230:1159–1170.
50. Macreadie, I.G., C.K. Arunagiri, D.R. Hewish, J.F. White, and A.A. Azad. 1996. Extracellular addition of a domain of HIV-1 Vpr containing the amino acid sequence motif H(S/F)RIG causes cell membrane permeabilization and death. *Mol. Microbiol.* 19:1185–1192.
51. Thorsness, P.E., K.H. White, and T.D. Fox. 1993. Inactivation of YME1, a member of the fts H-SEC18-PAZ1-CDC48 family of putative ATPase-encoding genes, causes increased escape of DNA from mitochondria in *Saccharomyces cerevisiae*. *Mol. Cell. Biol.* 13:5418–5426.
52. Macreadie, I.G., L.A. Castelli, D.R. Hewish, A. Kirkpatrick, A.C. Ward, and A.A. Azad. 1995. A domain of human immunodeficiency virus type 1 Vpr containing repeated H(S/F)RIG amino acid motifs causes cell growth arrest and structural defects. *Proc. Natl. Acad. Sci. USA*. 92:2770–2774.
53. Zhang, S., D. Pointer, G. Singer, Y. Feng, K. Park, and L.-J. Zhao. 1998. Direct binding to nucleic acids by Vpr of human immunodeficiency virus type 1. *Gene*. 212:157–166.
54. Piller, S.C., G.D. Ewart, D.A. Jans, P.W. Gage, and G.B. Cox. 1999. The amino-terminal region of Vpr from human immunodeficiency virus type 1 forms ion channels and kills neurons. *J. Virol.* 73:4230–4238.
55. Macreadie, I.G., D.R. Thorburn, D.M. Kirby, L.A. Castelli, N.L. Derozario, and A.A. Azad. 1997. HIV-1 protein Vpr causes gross mitochondrial dysfunction in the yeast *Saccharomyces cerevisiae*. *FEBS Lett.* 410:145–149.
56. Mancini, M., D.W. Nicholson, S. Roy, N.A. Thornberry, E.P. Peterson, L.A. Casciola-Rosen, and A. Rosen. 1998. The caspase-3 precursor has a cytosolic and mitochondrial distribution: implications for apoptotic signaling. *J. Cell Biol.* 140:1485–1495.
57. Lu, Y.L., P. Spearman, and L. Ratner. 1993. Human immunodeficiency virus type 1 viral protein R localization in intact cells and virions. *J. Virol.* 67:6542–6550.
58. Zhou, Y., Y. Lu, and L. Ratner. 1998. Arginine residues in

the C-terminus of HIV-1 Vpr are important for nuclear localization and cell cycle arrest. *Virology*. 242:414–424.
59. Westendorp, M.O., V.A. Shatrov, K. Schulze-Osthoff, R. Frank, M. Kraft, M. Los, P.H. Krammer, W. Dröge, and V. Lehrmann. 1995. HIV-1 Tat potentiates TNF-induced NF-κB activation and cytotoxicity by altering the cellular redox state. *EMBO (Eur. Mol. Biol. Organ.) J.* 14:546–554.
60. Strack, P.R., M.W. Frey, C.J. Rizzo, B. Cordova, H.J. George, R. Meade, S.W. Jo, J. Corman, R. Tritch, and B.D. Korant. 1996. Apoptosis mediated by HIV protease is preceded by cleavage of Bcl-2. *Proc. Natl. Acad. Sci. USA*. 93:9571–9576.
61. Macho, A., M. Castedo, P. Marchetti, J.J. Aguilar, D. Decaudin, N. Zamzami, P.M. Girard, J. Uriel, and G. Kroemer. 1995. Mitochondrial dysfunctions in circulating T lymphocytes from human immunodeficiency virus-1 carriers. *Blood*. 86:2481–2487.
62. Carbonari, M., M. Pesce, M. Cibati, A. Modica, L. Dellanna, G. Doffizi, A. Angelici, S. Uccini, A. Modesti, and M. Fiorilli. 1997. Death of bystander cells by a novel pathway involving early mitochondrial damage in human immunodeficiency virus-related lymphadenopathy. *Blood*. 90:209–216.
63. Frankel, A.D., and J.A.T. Young. 1998. HIV-1: fifteen proteins and an RNA. *Annu. Rev. Biochem*. 67:1–25.
64. Hrimech, M., X.-J. Yas, F. Bachand, N. Rougeau, and E.A. Cohen. 1999. Human immunodeficiency virus type 1 (HIV-1) Vpr functions as an immediate-early protein during HIV-1 infection. *J. Virol*. 73:4101–4109.
65. Tschopp, J., M. Thome, K. Hofmann, and E. Meinl. 1998. The fight of viruses against apoptosis. *Curr. Opin. Genet. Dev*. 8:82–87.
66. Evans, E.K., T. Kuwana, S.L. Strum, J.J. Smith, D.D. Newmeyer, and S. Kornbluth. 1997. Reaper-induced apoptosis in a vertebrate system. *EMBO (Eur. Mol. Biol. Organ.) J.* 16: 7272–7381.
67. Claveria, C., J.P. Albar, A. Serrano, J.M. Buesa, J.M. Barbero, A.C. Martinez, and M. Torres. 1998. Drosophila grim induces apoptosis in mammalian cells. *EMBO (Eur. Mol. Biol. Organ.) J.* 17:7199–7208.
68. Haining, W.N., C. Carboy-Newcomb, C.L. Wei, and H. Steller. 1999. The proapoptotic function of Drosophila Hid is conserved in mammalian cells. *Proc. Natl. Acad. Sci. USA*. 96: 4936–4941.